Inorganica Chimica Acta 375 (2011) 122–127

Contents lists available at ScienceDirect

Inorganica Chimica Acta

journal homepage: www.elsevier.com/locate/ica

Self-assembly of 1D metalloporphyrin array within pseudo-hexagonal channels of polyoxometalates

Amanda M. Smelser [a], Yan-Fen Li [a], Christopher N. Carmichael [a], Hou-Yin Zhao [a], Wei-Ping Pan [a], Sean Parkin [b], Bangbo Yan [a,*]

[a] Department of Chemistry, Western Kentucky University, 1906 College Heights Blvd, Bowling Green, KY 42101, USA
[b] Department of Chemistry, University of Kentucky, Lexington, KY 40506-0055, USA

ARTICLE INFO

Article history:
Received 7 October 2010
Received in revised form 21 April 2011
Accepted 22 April 2011
Available online 28 April 2011

Keywords:
Keggin cluster
Metalloporphyrin
Zinc complexes
Copper complexes
X-ray crystal structure
H-aggregation

ABSTRACT

Self-assembly of the robust Keggin cluster $[SiW_{12}O_{40}]^{4-}$ and metalloporphyrin building blocks $[M(TpyPH_n)]^{n+}$ under hydrothermal conditions gives two new organic–inorganic hybrid solid compounds. The hydrothermal reactions of $H_4SiO_4{\cdot}12WO_3{\cdot}xH_2O$, $Cu(NO_3)_2{\cdot}2.5H_2O$, *meso*-tetra(4-pyridyl)porphine (H_2TpyP) and H_2O at 200 °C for 72 h yield a solid compound $[Cu(TpyPH_3)]_2[Cu(TpyPH_2)][SiW_{12}O_{40}]_2{\cdot}8H_2O$ (**1**). Using $ZnCl_2$ instead of $Cu(NO_3)_2{\cdot}2.5H_2O$ in the syntheses leads to the crystallization of a compound $[Zn(TpyPH_4)(H_2O)][SiW_{12}O_{40}]{\cdot}3H_2O$ (**2**). Both compounds consist of discrete anionic α-$[SiW_{12}O_{40}]^{4-}$ clusters, cationic metalloporphyrins and crystalline water molecules. Hydrogen bonds, π–π aromatic interactions and CH···π interactions in these two new hybrid solids lead to the formation of 3D framework structures. Pseudo-hexagonal channels are formed by polyoxometalates and are occupied by one-dimensional metalloporphyrin arrays. Both compounds were characterized by single crystal X-ray, UV–Vis, IR spectroscopy and thermogravimetric analysis.

1. Introduction

Polyoxometalates (POM) are well-known for their great structural diversity and wide range of applications [1]. The photocatalytic properties of POMs have received specific attention due to their similarities to nano-sized TiO_2: i.e. rigid framework structures and abilities to accept and donate electrons, and their photocatalytic properties have been studied for many types of reactions [2,3]. However, POMs show low visible light photocatalytic activity and absorb mostly UV light which accounts for only a small fraction of solar energy. Therefore, approaches for the design of efficient heterogeneous POM-based photocatalytic materials have been developed by the association of ruthenium ion or its complexes with POMs [4]. We are interested in the combination of metalloporphyrin complexes with POMs in solid state to form materials with functionalized properties, especially photochemical properties. Since porphyrins have tunable photophysical and chemical properties, metalloporphyrins with different functionalities have been designed and can be used as building blocks in new hybrid solids [5]. However, hybrids solids containing both metalloporphyrins and POMs have been are rarely reported [6–11]. Most of the known hybrid solids containing both metalloporphyrins and POMs are involved in the interactions via covalent or coordination bonds between metalloporphyrin and POMs. Noncovalent interactions such as hydrogen bonds, CH···π and π–π are seldom studied for their role in the self-organization of metalloporphyrins with POMs.

In this report, we present our study on the self-assembly of the nano-sized Keggin ion $[SiW_{12}O_{40}]^{4-}$ with metalloporphyrin complexes ([M(TpyP)], M = Zn, Cu; H_2TpyP = *meso*-tetra(4-pyridyl) porphine) and the interactions between the Keggin clusters and metalloporphyrin in solid state. Hydrogen bonds, CH···π and π–π interactions lead to the formation of two new compounds: $[Cu(TpyPH_3)]_2[Cu(TpyPH_2)][SiW_{12}O_{40}]_2{\cdot}8H_2O$ (**1**) and $[Zn(TpyPH_4)(H_2O)][SiW_{12}O_{40}]{\cdot}3H_2O$ (**2**), with 3D networks.

2. Experimental

The reactions were carried out under hydrothermal autogenous pressure conditions using 3″ × 4″ Teflon bags in Teflon-lined stainless steel autoclave reactors. All chemicals were obtained from commercial sources and used without purification. No hazards were encountered in the experimental work reported. Reagents used included $H_4SiO_4{\cdot}12WO_3{\cdot}xH_2O$ (Alfa Aesar), *meso*-tetra (4-pyridyl)porphine (Frontier Scientific), $Cu(NO_3)_2{\cdot}2.5H_2O$

---

* Corresponding author. Tel.: +1 270 745 3943; fax: +1 270 7455361.
E-mail address: bangbo.yan@wku.edu (B. Yan).

0020-1693/$ - see front matter © 2011 Elsevier B.V. All rights reserved.
doi:10.1016/j.ica.2011.04.039

(Alfa Aesar), $ZnCl_2$ (Alfa Aesar). UV–Vis diffusion reflectance spectra were recorded on a Varian Cary 100 UV–Vis spectrophotometer equipped with the DRA-CA-30 Diffuse reflectance accessory. The infrared spectra were recorded from 400 to 4000 cm^{-1} on a Perkin–Elmer Spectrum One FTIR spectrometer using KBr pellets. The thermogravimetric data were collected on a TA Q5000 TGA instrument at a heating rate of 10 °C min^{-1} from room temperature to 800 °C in an air atmosphere.

*Compound **1***: $[Cu(TpyPH_3)]_2[Cu(TpyPH_2)][SiW_{12}O_{40}]_2 \cdot 8H_2O$ was prepared hydrothermally from a mixture of H_2TpyP, $H_4SiO_4 \cdot 12WO_3 \cdot xH_2O$, $Cu(NO_3)_2 \cdot 2.5H_2O$ and H_2O. A typical synthesis is as follow: 0.052 g H_2TpyP was dissolved in 1.30 mL H_2O by adjusting the pH to 0.9 using 2 M H_2SO_4. To this solution, $H_4SiO_4 \cdot 12WO_3 \cdot xH_2O$ (0.162 g) and $Cu(NO_3)_2 \cdot 2.5H_2O$ (0.019 g) were added. The pH of the resulting solution was adjusted with 2 M KOH to approximately 1.4, when no more purple precipitate formed. The reaction mixtures were transferred to a Teflon bag, sealed and placed in a 45 mL reaction vessel, and heated in an oven at 200 °C for 72 h. Dark red purple crystals were filtered and dried in air (yield: 0.15 g, 1.9×10^{-5} mol; 70% based on Cu). FT-IR spectrum (KBr, cm^{-1}): 3250 (broad), 3126, 3099, 3072, 1633, 1542, 1496, 971, 923, 886, 791.

*Compound **2***: $[Zn(TpyPH_4)(H_2O)][SiW_{12}O_{40}] \cdot 3H_2O$ was prepared using a similar method from a mixture of *meso*-tetra(4-pyridyl)porphine (0.052 g), $H_4SiO_4 \cdot 12WO_3 \cdot xH_2O$ (0.489 g), and $ZnCl_2$ (0.010 g). The pH of the resulting mixture was adjusted with 2 M KOH to ~1.4. The reaction mixtures were heated in an oven at 200 °C for 72 h. Dark red purple crystals were filtered and dried in air (yield: 0.13 g, 3.6×10^{-5} mol; 49% based on Zn). FT-IR spectrum (KBr, cm^{-1}): 3225, 3153, 3090, 1629, 1526, 1495, 973, 923, 883, 791.

2.1. Crystallography

X-ray diffraction data for compounds **1** and **2** were collected at 90.0(2) K on a Nonius kappa CCD diffractometer. Raw data were integrated, scaled, merged and corrected for Lorentz-polarization effects using the HKL-SMN package [12]. The structure was solved by direct methods and was refined against F^2 by weighted full-matrix least-squares calculations [13]. Hydrogen atoms of TpyP were placed at calculated positions and refined using a riding model except for the hydrogen atoms on nitrogen of pyridyl groups in **2**. No attempts were made to locate hydrogen atoms of water molecules from difference maps. Non-hydrogen atoms were refined with anisotropic displacement parameters. Atomic scattering factors were taken from the International Tables for Crystallography [14]. Crystal data and relevant details of the structure determinations are summarized in Table 1 and selected geometrical parameters are given in Table 2.

3. Results and discussions

The acidity of the initial reaction mixtures is critical for the crystallization of compounds **1** and **2**. When the pH of the initial reaction mixture is greater than 2, these two compounds cannot be crystallized. This is because H_2TpyP is insoluble in aqueous solution when pH is higher than about 2.5. Typically, the pH of the initial reaction mixture is 1.9, at which the pyridyl nitrogen atoms of H_2TpyP are expected to be bonded to hydrogen ions [15]. With the presence of metal ions of Cu and Zn, $[M(TpyPH_n)]^{n+}$ are expected to form in the solution. On the other hand, the Keggin ion in $H_4SiW_{12}O_{40}$ exists as $[SiW_{12}O_{40}]^{4-}$ in the solution [16]. The opposite charges on $[SiW_{12}O_{40}]^{4-}$ and $[M(TpyH_n)]^{n+}$, and hydrogen bond interactions play an important role in formation of these two compounds. The products were not soluble in common solvents such as water and methanol.

Table 1
Crystal data and structure refinements for **1**–**2**.

	1	**2**
Formula	$C_{120}H_{96}N_{24}Cu_3O_{88}Si_2W_{24}$	$C_{40}H_{36}N_8ZnO_{44}SiW_{12}$
Molecular weight	7941.4	3632.4
Crystal system	triclinic	triclinic
Space group	$P\bar{1}$	$P\bar{1}$
a (Å)	15.7454(1)	12.0354(2)
b (Å)	16.2062(1)	15.4881(3)
b (Å)	17.8423(2)	19.0080(4)
α (°)	97.9245(4)	68.920(1)
β (°)	94.9581(4)	89.071(1)
γ (°)	114.0847(4)	76.564(1)
V (Å^3)	4065.24(6)	3206.7(1)
Z	1	1
ρ (Mg m^3)	3.192	3.764
μ (mm^{-1})	17.39	21.92
Wavelength (Å)	0.71073	0.71073
Temperature (K)	90.0(2)	90.0(2)
Reflections collected/ unique (R_{int})	91558/18634	68763/14656
Goodness-of-fit(F^2)	1.017	0.975
Final R indices [$I > 2\sigma(I)$]	R_1 = 0.0390, wR_2=0.0867	R_1=0.0306, wR_2=0.0663
R indices (all data)	R_1=0.0696, wR_2=0.0981	R_1=0.0414, wR_2=0.0706

Table 2
Selected interatomic distances (Å) in compounds $[Cu(TpyPH_3)]_2[Cu(TpyPH_2)][SiW_{12}O_{40}]_2 \cdot 8H_2O$ (**1**) and $[Zn(TpyPH_4)(H_2O)][SiW_{12}O_{40}] \cdot 3H_2O$ (**2**).

	Compound **1**		Compound **2**	
	Range	Average	Range	Average
W–O_t	1.690(6)–1.716(6)	1.706	1.694(6)–1.718(6)	1.704
W–O_b	1.897(6)–1.980(6)	1.926	1.888(6)–1.949(6)	1.923
W–O_c	1.865(6)–1.943(6)	1.908	1.872(6)–1.942(6)	1.908
W–O_a	2.341(6)–2.372(6)	2.356	2.334(6)–2.368(6)	2.349
Cu(1)–N	1.990(7)–2.010(7)	1.999		
Cu(2)–N	2.008(8)–2.019(8)	2.014		
Zn(1)–N			2.048(6)–2.079(6)	2.060
Si–O	1.612(6)–1.628(6)	1.620	1.614(6)–1.628(6)	1.623

An X-ray diffraction analysis on a single crystal of compound **1** revealed its structure consists of α-$[SiW_{12}O_{40}]^{4-}$ cluster anions, lattice water molecules, and metalloporphyrin complexes. The α-$[SiW_{12}O_{40}]^{4-}$ Keggin anion consists of four W_3O_{13} groups, in which the three distorted WO_6 octahedra share a common oxygen atom [17]. The central Si atom coordinates to four common oxygen atoms from four W_3O_{13} groups to form the slightly distorted SiO_4 tetrahedron with Si–O bond lengths in the range of 1.612(6)–1.628(6) Å. There are four types of oxygen atoms (Table 2): terminal oxygen atoms O_t (W–O_t; 1.690(6)–1.716(6) Å); edge-bridging oxygen atoms O_c shared by two W atoms in the same W_3O_{13} group (W–O_c; 1.897(6)–1.980(6) Å); corner-bridging oxygen atoms O_b shared by two W atoms from different W_3O_{13} groups (W–O_b; 1.865(6)–1.943(6) Å), and central oxygen atoms O_a shared by three W atoms and one Si atom (W–O_a; 2.341(6)–2.372(6) Å). The Keggin ions are arranged in one-dimensional array along the *c* direction with the Si–Si distance of adjacent clusters at *ca.* 17.842(3) Å, which is much larger than the size of the cluster (~1 nm). The space between these Keggin clusters of the one-dimensional array is occupied by water molecules. The one-dimensional arrays of the anionic clusters are arranged such that pseudo hexagonal channels are formed (Fig. 1). The channels are occupied by copper metalloporphyrin complexes.

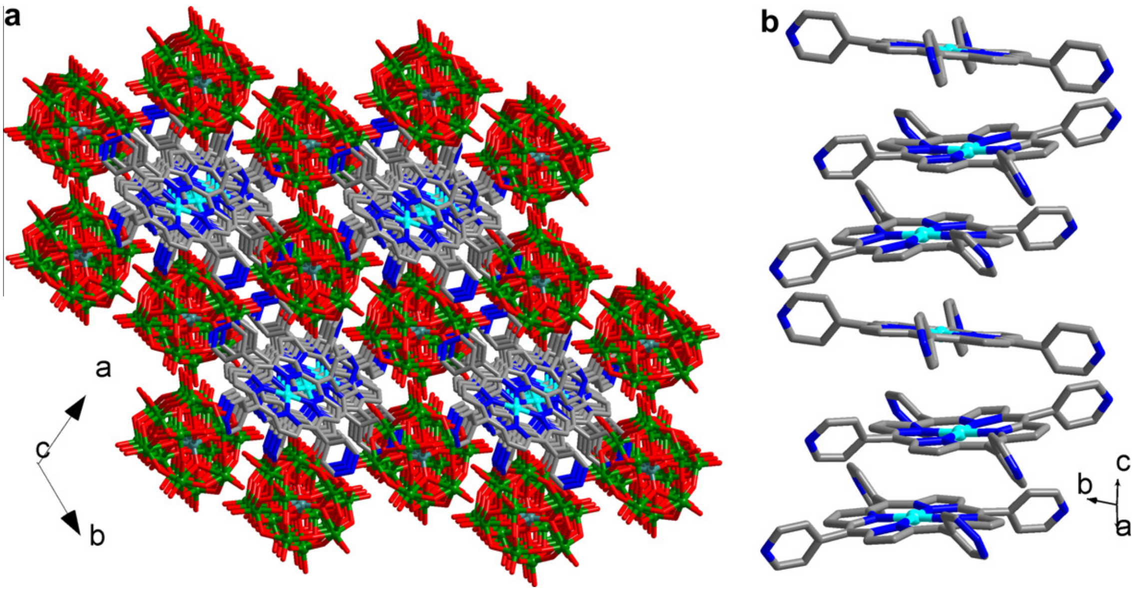

Fig. 1. (a) A representation of the pseudo hexagonal channels filled with 1D arrays of metalloporphyrins in **1**; (b) the one dimensional array of metalloporphyrins in **1**.

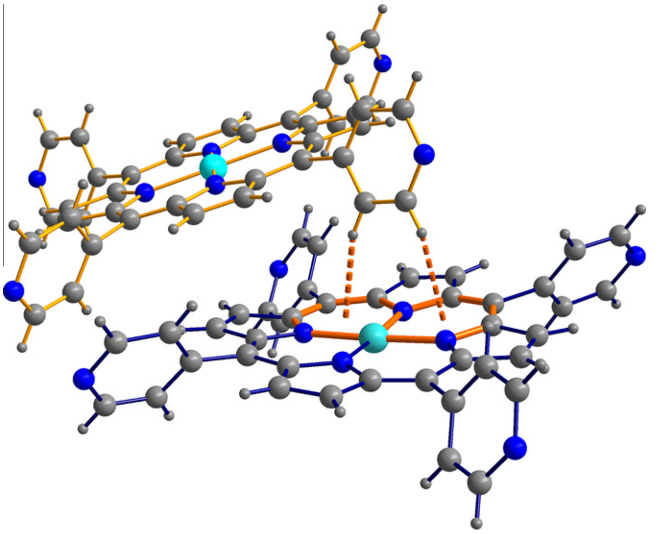

Fig. 2. A ball-and-stick representation of CH···π interaction (H-ring centroid distances: 2.44 Å, 2.75 Å) in **1**.

Adjacent copper metalloporphyrin complexes in **1** are stacked to form staircase-like one-dimensional arrays through π–π aromatic interactions and CH···π interactions (Fig. 2). There are two unique copper sites in **1**, both display a square planar $\{CuN_4\}$ coordination geometry (Cu–N: 1.990(7)–2.019(8) Å). These bond lengths are comparable to those in $[Cu(TpyP)Cu_2Mo_3O_{11}]$ [11b]. Two parallel metalloporphyrin complexes form a dimer through π–π aromatic interactions (with the face-to-face distance of ca. 3.83 Å). The 1D copper metalloporphyrin array is composed of $[Cu(TpyPH_3)]_2^{6+}$ dimers and $[Cu(TpyPH_2)]^{2+}$ monomers alternatively. These two types of copper metalloporphyrins are not parallel to each other (dihedral angle: 13.8°). But the C–H group of the pyridyl group from $[Cu(TpyPH_2)]^{2+}$ form CH···π interactions (H-ring centroid distances: 2.44 Å, 2.75 Å) with the π-system of a chelate ring formed by copper $[Cu(TpyPH_3)]_2^{6+}$ [18].

The 1D arrays of the metalloprophyrins are further extended into 3D frameworks via the intermolecular C–H···O hydrogen bonds between the Keggin anions and aromatic C–H groups (C···O 2.88(1)–3.51(1) Å, Table 3) [19]. Nitrogen atoms of pyridyl groups in the metalloprophyrins form two hydrogen bonds with two oxygen atoms of Keggin units $[SiW_{12}O_{40}]^{4-}$ (N9···O19: 2.64(1) Å; N10···O4: 2.73(1) Å, N11···O3w, 2.61(1) Å), and also with water molecule (N8···O2w: 2.96(1) Å).

Table 3
Geometrical parameters of selected hydrogen bonds (Å, °) for compound **1**.

D–H···A	d(D–H)	d(H···A)	d(D···A)	∠DHA
C(7)–H(7A)···O(37)	0.95	2.57	3.51	168
C(11)–H(11A)···O(6)	0.95	2.57	2.98	106
C(13)–H(13A)···O(22)	0.95	2.55	2.91	102
C(18)–H(18A)···O(18)	0.95	2.55	3.49	169
C(23)–H(23A)···O(8)	0.95	2.21	2.88	127
C(28)–H(28A)···O(26)	0.95	2.21	3.14	165
C(30)–H(30A)···O(22)	0.95	2.47	3.23	143
C(35)–H(35A)···O(7)	0.95	2.54	3.22	129
C(41)–H(41A)···O(37)	0.95	2.45	3.33	154
O(2w)–H...N(8)	–	–	2.96	–
O(3w)–H...N(11)	–	–	2.61	–
N(10)–H ···O(4)	–	–	2.73	–

In forming metalloporphyrin complexes, copper(II) generally has four-coordination preference [11], while zinc prefers five-coordinated square pyramidal geometry [20]. To investigate the influence of metal ions on the packing of metalloporphyrins within channels of POMs, Zn(II) ion was used in the synthesis. Using $ZnCl_2$ instead of $Cu(NO_3)_2 \cdot 2.5H_2O$ in the syntheses led to the crystallization of compound $[Zn(TpyPH_4)(H_2O)][SiW_{12}O_{40}] \cdot 3H_2O$ (**2**). Single crystal X-ray analysis on the structure of 2 reveals that it consists of anionic α-$[SiW_{12}O_{40}]^{4-}$ clusters, cationic $[Zn(TpyPH_4)(H_2O)]^{4+}$ and crystalline water molecules. The Keggin ion α-$[SiW_{12}O_{40}]^{4-}$ of **2** is almost identical to that of **1** (Table 2). Similar to compound **1**, α-$[SiW_{12}O_{40}]^{4-}$ clusters form pseudo hexagonal channels with 1D array of π–π stacked $[Zn(TpyPH_4)(H_2O)]^{4+}$ metalloporphyrin arrays occupying the channels (Fig. 3). However, in **2**, there is only one unique zinc site, which exhibits square-pyramidal coordination geometry with a water molecule at the axial position (Zn–N 2.048(6)–2.079(6), Zn–O: 2.137(6) Å). The zinc atom is located slightly above the basal plane (0.253(1) Å from the basal plane). The π–π aromatic stacking and CH···π interactions between $[Zn(TpyPH_4)(H_2O)]^{4+}$ units led to the formation of zinc metalloporphyrin dimers with the two square pyramidal {ZnN_4O} units packed back to back.

Stronger CH···π (H-ring centroid distances: 2.49 Å, 2.86 Å) and π–π aromatic stacking interactions (face-to-face distance of ca. 3.94 Å) between zinc metalloporphyrins within the dimer than those in adjacent dimers are observed (Fig. 4), mainly because of the hindrance of coordinated water molecules. Two nitrogen atoms of the four pyridyl groups in $[Zn(TpyPH_4)(H_2O)]^{4+}$ forms hydrogen bonds with two oxygen atoms of the anionic cluster (N8···O39, 2.79 Å; N2···O4, 2.90 Å, see Table 4). The rest two nitrogen atoms form hydrogen bonds with water molecules. Again, the 1-D arrays of the prophyrins are further extended into 3-D frameworks via the intermolecular C–H···O hydrogen bonds between the cluster oxygen atoms and aromatic C–H groups (C···O 3.10(1)–3.38(1) Å).

The π-stacking interaction energy of metalloporphyrin aggregations is about the same of classic hydrogen bonds [19]. The structures of compounds **1** and **2** indicate that the noncovalent interactions between POMs and metalloporphrins play an important role in the self-assembly of these frameworks. The results suggest that 3-D structures are due to both H-bonds along the porphyrin plane, π-stacking interactions in the axial direction and CH···π interactions [21]. Our results also showed that weak hydrogen bonds such as CH···O also play a significant role in the crystal packing and crystal engineering [22].

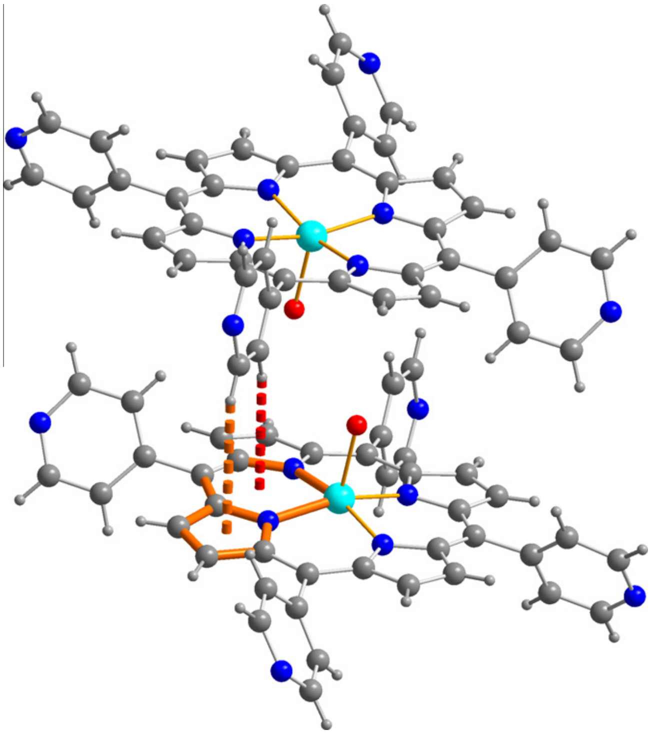

Fig. 4. A ball-and-stick representation of CH···π interaction (H-ring centroid distances: 3.01 Å, 3.58 Å) in **2**.

Since the $H_4SiW_{12}O_{40}$ is a very strong acid (stronger than H_2SO_4) [23], it is reasonable to expect the α-$[SiW_{12}O_{40}]^{4-}$ ion does not bond to any hydrogen ion in the solid crystallized from the acidic reaction mixtures (pH ~2). Although, there are no reports in the literature on the pK_a values for the protonation of the peripheral pyridyl moieties in TpyP, the pK_a of TpyP for the first protonation step of the inner nitrogen atoms of the pyrrole ring is measured to be 1.8 [24]. Moreover, in acidic solution the peripheral pyridyl nitrogen will be protonated first [25]. Thus the peripheral pyridyl hydrogen is weaker than $H_4SiW_{12}O_{40}$ and would be protonated before $[SiW_{12}O_{40}]^{4-}$. Bond valence sum calculations show all tungsten atoms are at their highest oxidation states (6+) in **1** and **2** [26]. To balance the negative charges on α-$[SiW_{12}O_{40}]^{4-}$, pyridyl groups of the metalloporphyrin complexes need to be protonated. In fact, under the reaction conditions, this is very likely to happen. We cannot determine the H^+ ions on the pyridyl groups for **1** from its crystal data, and we can locate only two H^+ ions on nitrogen atoms of pyridyl groups for **2**. The pyridyl groups in **1** are partially protonated and all pyridyl groups are protonated in

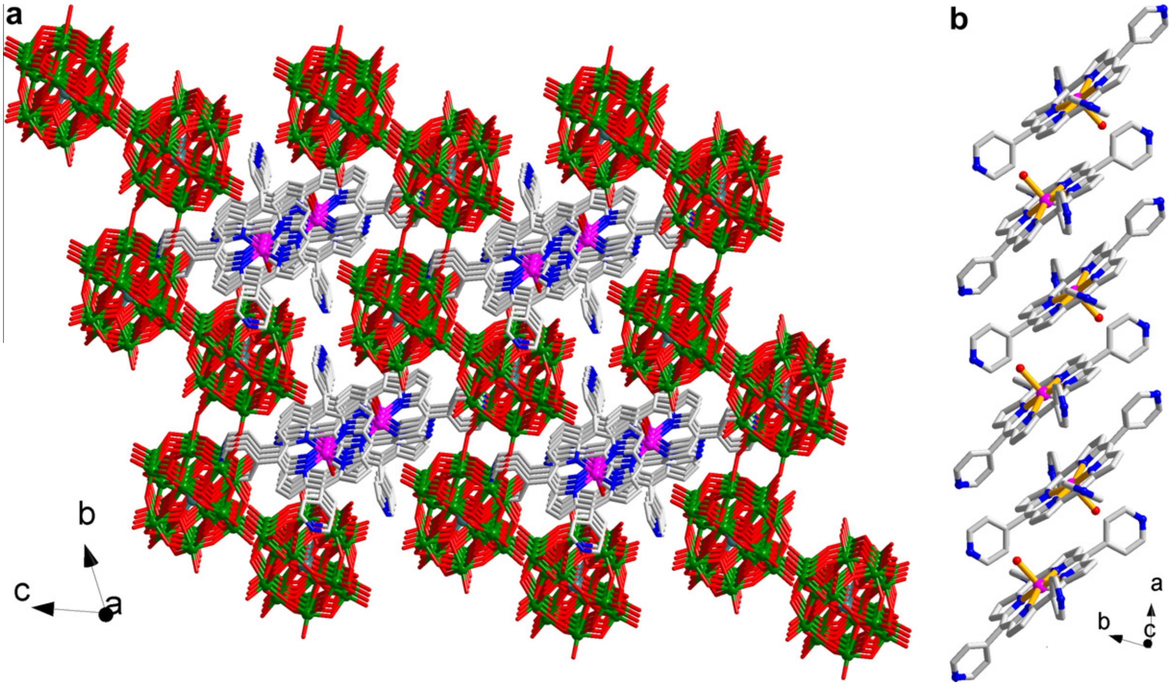

Fig. 3. (a) Polyhedral and space-filling representation of the pseudo hexagonal channels filled with 1D arrays of metalloporphyrins in **2**; (b) the one dimensional array of metalloporphyrins in **2**.

Table 4
Geometrical parameters of selected hydrogen bonds (Å, °) for compound **2**.

D–H···A	d(D–H)	d(H···A)	d(D···A)	∠DHA
N8–H1PY···O39	0.69	2.28	2.7933	132
N2–H2PY···O4	0.8	2.38	2.9026	124
N2–H2PY···O7	0.8	2.41	3.1138	147
N2–H2PY···O9	0.8	2.35	2.9925	138
C59–H59A···O27	0.93	2.47	3.0988	125
C60–H60A···O37	0.93	2.4	3.1167	134
C69–H69A···O2W	0.93	2.59	3.2191	125
C70–H70A···O29	0.93	2.53	3.2594	135
C71–H71A···O9	0.93	2.33	3.1042	141
C73–H73A···O29	0.93	2.36	3.2865	172
C86–H86A···O37	0.93	2.51	3.172	128
C90–H90A···O31	0.93	2.58	3.3798	144

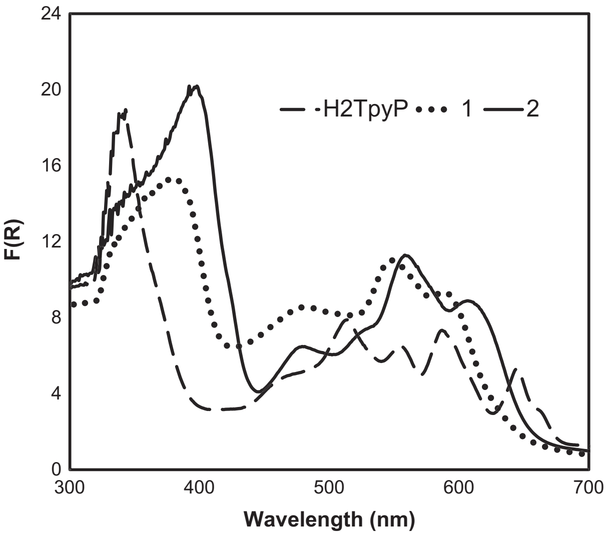

Fig. 5. UV–Vis diffuse reflectance spectra of H_2TpyP (dash line), compound **1** (dotted line), and compound **2** (solid line).

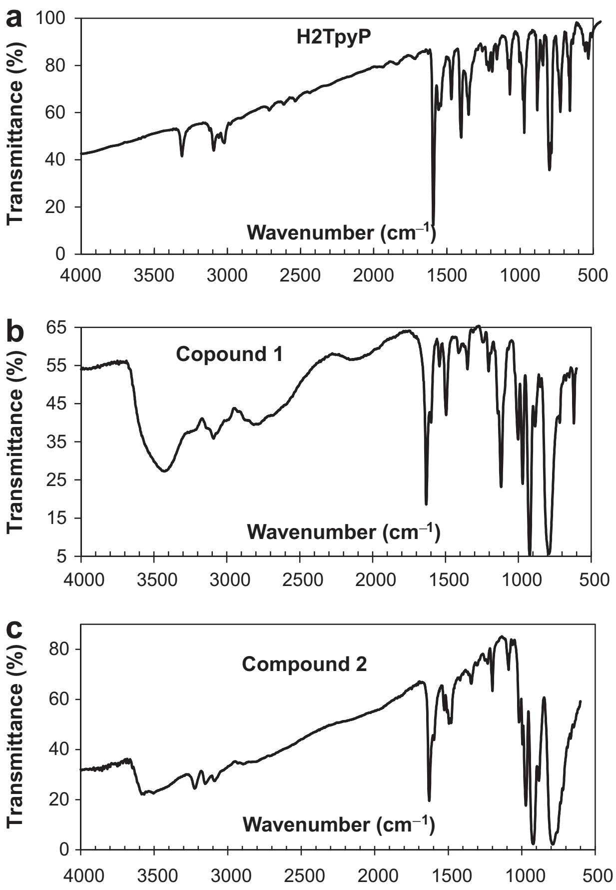

Fig. 6. IR spectra of (a) H_2TpyP, (b) compound **1**, and (c) compound **2**.

2. The protonation of pyridyl groups is also confirmed by IR spectra.

Fig. 5 displays the UV–Vis diffuse reflectance spectra of H_2TpyP, **1** and **2**. The diffuse reflectance spectrum of H_2TpyP displays the strong Soret band (or B band) at 340 nm and four Q bands at 514, 555, 587, and 644 nm. This Soret band is consistent with the calculated value (344 nm) without considering the solvent effects [27]. The blue shift of the Soret band for solid H_2TpyP in compare with the Soret band of H_2TpyP in aqueous solution (420 nm) [28] can be attributed to the lack of solvent effects in solids. The Q bands of solid H_2TpyP do not change significantly in compare with those of H_2TpyP in solutions. The diffuse reflectance spectrum of **1** shows a broad Soret band with maximum at around 384 nm, and three Q bands peaks at 481, 548 and 589 nm. Similarly, **2** shows a broad Soret band at around 398 nm and three Q bands peaks at 479, 558 and 603 nm. The red shift of the Soret bands in **1** and **2** in compare with those of solid H_2TpyP is because of the coordination of metal ions to form the complexes [29]. The most notable features of the spectra of **1** and **2** are that the Soret band maxima are blue shifted with respect to ZnTpyP (438 nm) and CuTpyP (416 nm). Such behavior could be attributed to the formation of H-aggregates (face-to-face stacking) between porphyrin molecules in crystal structures [30]. A blue-shift of Soret band is consistent with a parallel stacking of the porphyrin molecules due to excitonic coupling of the electronic transitions in the porphyrin π-systems [31]. It is known that the J-aggregate generally displays an intense and narrow absorption band [32], while the higher self-aggregates without J-type arrangement exhibit a broad Soret band. The Soret bands in **1** and **2** are broad at 323–424 nm, and 323–445 nm, respectively, in contrast to the sharp Soret band for H_2TpyP. It is however should be pointed out that about a half of a porphyrin ring overlaps another in the dimer unit of **1** and this overlap is less than a quarter in the dimer unit of **2**.

The infrared spectra of H_2TpyP, **1** and **2** are shown in Fig. 6. The vibration bands at 3120–3300 cm^{-1}, which can be assigned to N–H vibrations (broad band at 3215–3290 cm^{-1} for **1**, and 3225 cm^{-1} for **2**), demonstrate the presence of protonated pyridyl groups in **1** and **2**. The shift to lower wavenumbers of these N–H vibrations bands is because of the hydrogen bonding involved in the N–H groups. The N–H vibrations might overlap with the C–H stretching vibrations, which are located at 3040–3190 cm^{-1}. The metal-free H_2TpyP shows 3021 and 3093 cm^{-1} for the stretching vibrations of C–H. The bands at 1630 cm^{-1} due to stretching vibrations of C=C in the pyridyl aromatic ring show a blue shift in **1** and **2** compared to H_2TpyP (1594 cm^{-1}). Both compounds show characteristic bands for $[SiW_{12}O_{40}]^{4-}$, namely, $\nu(W–O_t)$, $\nu(Si–O_a)$, $\nu(W–O_b)$ and $\nu(W–O_c)$ at 971, 923, 886 and 791 cm^{-1}, for **1**, and at 973, 923, 883 and 791 cm^{-1} for **2** [33]. However, the $\nu(W–O_c)$ overlaps with C–H vibrations of pyrrol which is located at 793 cm^{-1} in ZnTpyP and the band of $\nu(W–O_b)$ overlaps with a band from ZnTpyP.

Thermogravimetric analysis of compound **1** exhibits a 2.2% weight loss in the range 40–250 °C, followed by 25.0% weight loss between 400–700 °C. These correspond to the loss of water molecules (*calcd.* 2.27%) and porphyrins (*calcd.* 23.9%). Compound **2** shows similar thermogravimtric behavior: a weight loss of 2.2%

(*calcd.* 2.5%) in 40–200 °C, and a weight loss of 16.9% (*calcd.* 17.0%) at the range of 400–700 °C.

4. Conclusion

In summary, we have prepared and characterized two new hybrid framework solids based on POMs and metalloporphyrins connected through hydrogen bonds, π–π and CH···π interactions. Hydrogen bonds are believed to play an important role in biological electron transport, and it is found that hydrogen bond interface would provide greater electronic coupling than C–C σ bonds [22]. It has been shown the excited state resident on the porphyrin is capable of transferring an electron to the POM [6]. Compounds **1** and **2** provide new examples with 1D array of porphyrins linked to POMs. These systems may have the potential of interesting photocatalytic properties, and related research is underway.

Acknowledgments

We are grateful for financial support from internal grant of WKU, NSF EPSCoR (4800001974), and KY EPSCoR (RSF-030-06).

Appendix A. Supplementary material

CCDC 785408 and 785409 contain the supplementary crystallographic data for compounds **1** and **2**, respectively. These data can be obtained free of charge from The Cambridge Crystallographic Data Centre via www.ccdc.cam.ac.uk/data_request/cif. Supplementary data associated with this article can be found, in the online version, at doi:10.1016/j.ica.2011.04.039.

References

[1] (a)M.T. Pope, A. Müller (Eds.), Polyoxometalate Chemistry from Topology via Self-Assembly to Applications, Kluwer Academic Publishers, Dordrecht, 2001;
(b) D.L. Long, E. Burkholder, L. Cronin, Chem. Soc. Rev. 36 (2007) 105;
(c) A. Proust, R. Thouvenot, P. Gouzerh, Chem. Commun. (2008) 1837;
(d) C.-Y. Sun, S.-X. Liu, D.-D. Liang, K.-Z. Shao, Y.-H. Ren, Z.-M. Su, J. Am. Chem. Soc. 131 (2009) 883;
(e) J. Zhang, J. Hao, Y.G. Wei, F.P. Xiao, P.C. Yin, L.S. Wang, J. Am. Chem. Soc. 132 (2010) 14;
(f) P. Mialane, A. Dolbecq, F. Sécheresse, Chem. Commun. (2006) 3477;
(g) A. Sartorel, M. Carraro, G. Scorrano, R. De Zorzi, S. Geremia, N.D. McDaniel, S. Bernhard, M. Bonchio, J. Am. Chem. Soc. 130 (2008) 5006;
(h) K. Kamata, K. Yonehara, Y. Sumida, K. Yamaguchi, N. Mizuno, Science 300 (2003) 964.

[2] (a) E. Papaconstantinou, Chem. Soc. Rev. 18 (1989) 1;
(b) N. Mizuno, M. Misono, Chem. Rev. 98 (1998) 199;
(c) H. Yang, T. Liu, M. Cao, H. Li, S. Gao, R. Cao, Chem. Commun. 46 (2010) 2429;
(d) R. Neumann, A.M. Khenkin, Chem. Commun. (2006) 2529;
(e) R.C. Chambers, C.L. Hill, J. Am. Chem. Soc. 112 (1990) 8427;
(f) S. Kim, H. Park, W. Choi, J. Phys. Chem. B 108 (2004) 6402;
(g) A. Hiskia, A. Mylonas, E. Papaconstantinou, Chem. Soc. Rev. 30 (2001) 62.

[3] (a) R. Akid, J.R. Darwent, J. Chem. Soc., Dalton Trans. (1985) 395;
(b) Y. Li, C. Ren, S. Peng, G. Lu, S. Li, J. Mol. Catal. A: Chem. 246 (2006) 212;
(c) T. Yamase, R. Watanabe, J. Chem. Soc., Dalton Trans. (1986) 1699;
(d) J.R. Darwent, J. Chem. Soc., Chem. Commun. (1982) 798.

[4] (a) Y.V. Geletii, B. Botar, P. Kogerler, D.A. Hillesheim, D.G. Musaev, Craig L. Hill, Angew. Chem., Int. Ed. 47 (2008) 3896;
(b) A. Sartorel, M. Carraro, G. Scorrano, R. De Zorzi, S. Geremia, N.D. McDaniel, S. Bernhard, M. Bonchio, J. Am. Chem. Soc. 130 (2008) 5007.

[5] (a) D. Gust, T.A. Moore, A.L. Moore, Acc. Chem. Res. 34 (2001) 40;
(b) E. Iengo, E. Zangrando, E. Alessio, Acc. Chem. Res. 39 (2006) 841;
(c) I. Beletskaya, V.S. Tyurin, A.Y. Tsivadze, R. Guilard, C. Stern, Chem. Rev. 109 (2009) 1659;
(d) N. Zheng, J. Zhang, X. Bu, P. Feng, Cryst. Growth Des. 7 (2007) 2576.

[6] A. Harriman, K.J. Elliott, M.A.H. Alamiry, L.L. Pleux, M. Severac, Y. Pellegrin, E. Blart, C. Fosse, C. Cannizzo, C.R. Mayer, F. Odobel, J. Phys. Chem. C 113 (2009) 5834.

[7] C. Allain, S. Favette, L.-M. Chamoreau, J. Vaissermann, L. Ruhlmann, B. Hasenknopf, Eur. J. Inorg. Chem. (2008) 3433.

[8] A. Yokoyama, T. Kojima, K. Ohkubo, S. Fukuzumi, Chem. Commun. (2007) 3997.

[9] A. Tsuda, E. Hirahara, Y.-S. Kim, H. Tanaka, T. Kawai, T. Aida, Angew. Chem., Int. Ed. 43 (2004) 6327.

[10] C. Costa-Coquelard, S. Sorgues, L. Ruhlmann, J. Phys. Chem. A 114 (2010) 6394.

[11] (a) D. Hagrman, P.J. Hagrman, J. Zubieta, Angew. Chem., Int. Ed. 39 (1999) 3165;
(b) G. Yucesan, V. Golub, C.J. O'Connorb, J. Zubieta, CrystEngComm 6 (2004) 323.

[12] Z. Otwinowski, W. Minor, in: C.W. Carter Jr., R.M. Swet (Eds.), Macromolecular Crystallography Part A, vol. 276, Academic Press, 1997, p. 307.

[13] G.M. Sheldrick, Acta Crystallogr., Sect. A 64 (2008) 112.

[14] Th. Hahn (Ed.), International Tables for Crystallography, vol. C, Kluwer Academic Publishers, Holland

[15] E.B. Fleischer, L.E. Webb, J. Phys. Chem. 67 (1963) 1131.

[16] M.N. Timofeeva, G.M. Maksimov, V.A. Likholobov, Kinet. Catal. 42 (2001) 30.

[17] A. Kobayashi, Y. Sasaki, Bull. Chem. Soc. Jpn. 48 (1975) 885.

[18] G.A. Bogdanovic, A. Spasojevic-de Bire, S.D. Zaric, Eur. J. Inorg. Chem. (2002) 1599.

[19] (a) M. Du, Z.-H. Zhang, X.-J. Zhao, Cryst. Growth Des. 5 (2005) 1199;
(b) I.D.H. Oswald, W.D.S. Motherwel, Simon Parsonsa, Acta Crystallogr., Sect. B 61 (2005) 46;
(c) T. Steiner, Angew. Chem., Int. Ed. 41 (2002) 48.

[20] (a) Y. Diskin-Posner, S. Dahal, I. Goldberg, Angew. Chem., Int. Ed. 39 (2000) 1288;
(b) L. Carlucci, G. Ciani, D.M. Proserpio, F. Porta, Angew. Chem., Int. Ed. 42 (2003) 317.

[21] (a) I. Radivojevic, I. Likhtina, X. Shi, S. Singh, C.M. Drain, Chem. Commun. 46 (2010) 1643;
(b) Y. Jiang, C. Xi, Y. Liu, J. Niclos-Gutierrez, D. Choquesillo-Lazarte, Eur. J. Inorg. Chem. (2005) 1585.

[22] G.R. Desiraju, Acc. Chem. Res. 35 (2002) 565.

[23] I.V. Kozhevnikov, Chem. Rev. 98 (1998) 171.

[24] K. Kalyanasundaram, Inorg. Chem. 23 (1984) 2453.

[25] G.D. Luca, A. Romeo, L.M. Scolaro, J. Phys. Chem. B 109 (2005) 7149.

[26] I.D. Brown, D. Alternatt, Acta Crystallogr., Sect. B 41 (1985) 244.

[27] P. Yao, S. Han, Y. Zhang, X. Zhang, J. Jiang, Vib. Spectrosc. 50 (2009) 169.

[28] E.B. Fleischer, Inorg. Chem. 1 (1962) 493.

[29] A. Stone, E.B. Fleischer, J. Am. Chem. Soc. 90 (1968) 2735.

[30] R.F. Khairutdinov, N. Serpone, J. Phys. Chem. B 103 (1999) 761.

[31] M. Adachi, M. Yoneyama, S. Nakamura, Langmuir 8 (1992) 2240.

[32] K. Kano, K. Fukuda, H. Wakami, R. Nishiyabu, R.F. Pasternack, J. Am. Chem. Soc. 122 (2000) 7494.

[33] C. Rocchiccioli-Deltcheff, M. Fournier, R. Franck, R. Thouvenot, Inorg. Chem. 22 (1983) 207.